Interface bonding and manipulation of Ag and Cu nanocrystals on Si(111)-(7×7)-based surfaces

S. Jay Chey, L. Huang, and J. H. Weaver
Department of Materials Science and Chemical Engineering, University of Minnesota, Minneapolis, Minnesota 55455
(Received 13 July 1998)

Clusters of pure Ag, pure Cu, and mixed Ag-Cu were grown on solid Xe at 50 K. Subsequent desorption of the Xe buffer layers delivered the nanocrystals to pristine Si(111)-(7×7). Imaging with scanning tunneling microscopy showed that these structures ranged in size from 100 to 40 000 atoms. We investigated their interactions and bonding with the surface, and attempted to manipulate them on the surface using the tip of the scanning tunneling microscope. Silver nanocrystals could be pushed by mechanical contact, and they left behind a Ag track due to site-selective Ag-atom transfer to the surface. Copper nanocrystals could not be moved but they could be sheared by tip contact. Composite Ag-Cu nanocrystals could be pushed on Si(111) for low Cu contents, though adhesive interactions with the surface tended to separate the constituents. These results are discussed in terms of the bonding with the surface, the tendency to form necks with the tip, and the dynamics of particle movement. For Ag nanostructures, we also examined interface formation and manipulation on Ag(111), on Si(111)-($\sqrt{3}\times\sqrt{3}$) Ag, and on Br-exposed and adsorbate-decorated Si(111)-(7×7).
[S0163-1829(99)06224-4]

INTRODUCTION

The manipulation and assembly of nanoscale objects is a topic of considerable current interest. Several authors have shown that individual atoms and small molecules can be positioned with atomic scale accuracy using the tip of a scanning tunneling microscope (STM).[1–5] Others have demonstrated manipulation of weakly bound clusters on surfaces via mechanical contact with the tip of an atomic force microscope (AFM).[6] It is also possible to fabricate nanofeatures with the tip by field evaporation,[7] by electron-induced desorption,[8] and by enhanced surface diffusion.[9] Recently, we demonstrated the concept of ''nanopainting,'' using the STM tip to manipulate Ag particles containing up to $\sim 10^5$ atoms on clean Si(111)-(7×7).[10]

In this paper, we discuss the manipulation of nanostructures derived from 100 to 40 000 atoms. The nanostructures are pure Ag, pure Cu, and mixed Ag-Cu, and the surfaces are Si(111)-(7×7), Si(111)-($\sqrt{3}\times\sqrt{3}$) Ag, Ag(111), and adsorbate-exposed Si(111). Silver and copper were chosen because they have different bonding characteristics with Si(111)-(7×7) and different tendencies to bond with the tungsten tip. Most of the measurements were performed in ultrahigh vacuum (operating pressure $<5\times10^{-11}$ Torr) to maintain a clean environment where impurities would not change the adhesive properties. Others were done after intentional exposure to assess changes in interface bonding. We discuss behaviors that include weak, intermediate, and strong substrate bonding, manipulation with adhesive wear, particle lift-off, particle shearing, and particle coarsening. Throughout the discussion, we focus on the atomic-scale structure and bonding at the interfaces between the particle and the surface and between the particle and the tip.

EXPERIMENT

These studies were made possible by our buffer-layer-assisted growth technique[11,12] whereby three-dimensional (3D) structures of variable size could be deposited onto a selected substrate. Nanocrystal formation and delivery was done as follows. Clean Si(111)-(7×7) samples were prepared and characterized in the STM measurement chamber before transfer to a connected chamber where they were cooled to 50 K using a closed-cycle helium refrigerator. Subsequent exposure to ultrapure Xe resulted in the growth of a buffer layer whose thickness was estimated from the Xe pressure and exposure time.[13] The buffered sample was then exposed to a flux of Ag or Cu atoms from thermal sources (deposition rate ~0.6 Å/min). These metal atoms were sufficiently mobile on Xe that they formed clusters.[11] Composite samples derived from Ag and Cu were prepared by depositing Ag and then Cu on the buffer layer. Desorption of the buffer layer occurred when the samples were removed from the cold stage by a transfer fork. The desorption process agitates the clusters and, depending on the Xe layer thickness, the clusters contact each other and coalesce before reaching the pristine Si surface.[12] Imaging was done at room temperature under conditions that minimized the influence of the tip, namely, slow scan rates with +2.0-V sample bias and 0.2-nA current. Manipulation was done under different conditions, as discussed below.

RESULTS AND DISCUSSION

Contact between the growing clusters and Si(111)-(7×7) is established as Xe desorbs at ~90 K. The atomic-level details of the contact will depend on the chemistry of the constituents and the constraints imposed by kinetics. Thus we should expect different systems to exhibit different tendencies to wet or to modify the surface region. For example, we would expect Ag particles to wet Ag(111) because of the high diffusivity of Ag on Ag, and we show that this is the case. For nanostructures of Si, however, there are higher barriers associated with changes in shape and wetting would be unlikely at 300 K and below. As far as reaction is concerned, photoemission studies of transition metal clusters delivered

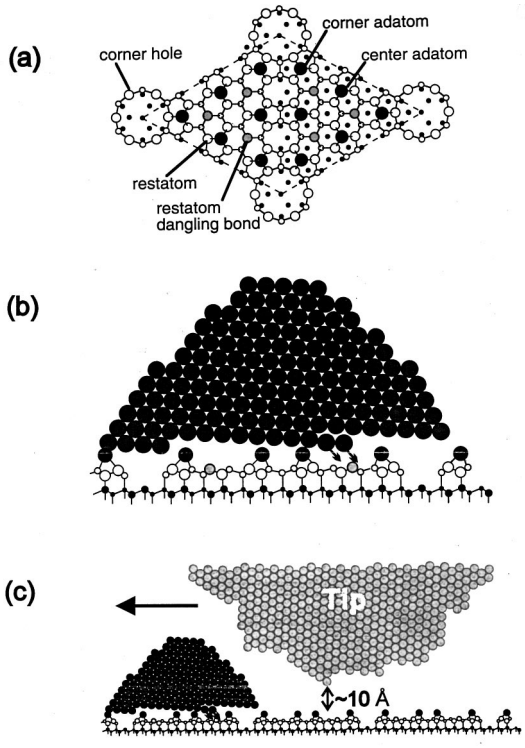

FIG. 1. (a) Model of the Si(111)-(7×7) surface showing adatoms and rest atoms that have dangling bonds and are the sites of greatest chemical affinity. Atoms of the corner holes are fully coordinated and are inert. (b) Representation of a Ag nanostructure formed by buffer-layer-assisted growth and cluster coalescence. It is approximately hemispherical and would be made up of ~2000 atoms. Contact with the surface implies kinetically restricted structural changes and bond formation that includes site-selective transfer of atoms to active sites of the Si surface. Crystallinity is implied, though the sketch is not crystallographically rigorous. (c) Depiction of a STM tip with close-packed atoms that is about to make mechanical contact with a Ag nanostructure. The nanostructures will move with the tip if bonding to the substrate is not too great. It will be transferred to the tip if a neck is formed with a strength that exceeds the substrate attraction.

to GaAs(110) and InP(110) showed minimal disruption of the surface, as judged by the absence of states in the gap and Fermi level movement.[11] Photoemission studies of metal clusters delivered to $YBa_2Cu_3O_x$ showed surface layer reaction driven by thermodynamics but this reaction was much less than that seen for atom-by-atom deposition because of kinetic stabilization at 300 K.[11]

Figure 1 helps to visualize the contact between a Ag nanocrystal and Si(111)-(7×7). Figures 1(a) and 1(b) show the characteristic features of clean Si(111)-(7×7). The cross section in Fig. 1(b) corresponds to a line drawn between the corner holes. The top, or adatom, layer has a very low planar density. Dangling bonds of this layer and the rest-atom layer tend to be chemically active with adsorbates. Atoms of the corner holes are fully coordinated and relatively inert. The (diagonal) center-to-center distance between corner holes is 46.6 Å. This is about 16 times the nearest-neighbor separation for Ag, 2.89 Å. The cross section in Fig. 1(b) for Ag is drawn close packed for simplicity. If it were hemispherical,[11] it would contain ~2000 atoms. Since nucleation on the buffer layer produces clusters with a mean size of ~28 atoms,[12] this object would have grown by coalescence from ~70 clusters. Upon contact with Si, it would have changed shape to optimize interface bonding and to minimize its surface energies. The base of the Ag particles is drawn as stepped to emphasize contact irregularity, and Ag atoms are depicted as moving to the Si rest-atom sites. The contact is then laterally inhomogeneous on the scale of the 7×7 unit cell, as will be discussed in more detail below for both Ag and Cu.

Figure 1(c) depicts a Ag nanostructure that is about to establish mechanical contact with a hypothetical STM tip. (For simplicity, the cross section represents a close-packed structure, though our tips were bcc.) Contact with the shank rather than the active tip is implied since the radius of the curvature for a tip may be ~1000 Å, and that of the particle may be 50 Å. During manipulation, two competing processes must be considered, and both are dynamic. One involves bonding with the substrate and the other involves bond formation with the tip. Manipulation on the surface can occur if tip wetting does not occur and substrate bonding is weak.[6] Wetting will be favored if the surface energy of the tip is high and that of the particle is low. This tip wetting is analogous to what occurs when the particle wets the substrate after Xe desorption. If a strong neck is formed and substrate bonding is weak, then the particle may transfer to the tip. In this case, imaging with STM will be unstable. Nanomanipulation will then be sensitive to the details of the bonding at the two contacts and the dynamics associated with atom diffusion and structural changes.

From Fig. 1(c), the size of the nanostructure determined by (noncontact) STM imaging would reflect the convolution with the tip, making it appear larger than it is.[14] On the other hand, the height relative to the surface would be determined more reliably, and we use this height in characterizing a particle's size. The assumption in estimating the number of atoms in a particle is that it is hemispherical in shape. Support for this simplification comes from photoemission studies that related the cluster size to its ability to attenuate the signal from the substrate beneath it.[15] Estimates of the total cluster volume on the surface agree with measurements using a quartz-crystal oscillator adjacent to the sample during deposition. Finally, when Ag nanostructures can be moved, we see track widths that are approximately twice the measured height, in agreement with the hemispherical particle picture.

Ag nanocrystals and Si(111)

Figure 2 shows several nanocrystals produced after depositing 1.3 Å of Ag onto a 60-ML Xe layer on Si(111)-(7×7). A step crosses the image. The rectangular box demonstrates that the 7×7 reconstruction persists after Xe sublimation, as expected, and that there is no contamination (obtained with +2-V sample bias and 0.7-nA tunneling current). From larger-size images, the Ag island density is 2.8×10^{10} cm^{-2} and the heights vary from 9 to 70 Å (100–40 000 atoms). Structure I in Fig. 2 is ~27 Å high, approximately the size of the particle represented in Fig. 1(b). Structure II is irregular and appears to have been formed from contact of two intermediate-sized objects. It may be changing shape slowly due to on-cluster Ag diffusion. Shape changes can be enhanced by repeated scanning at higher cur-

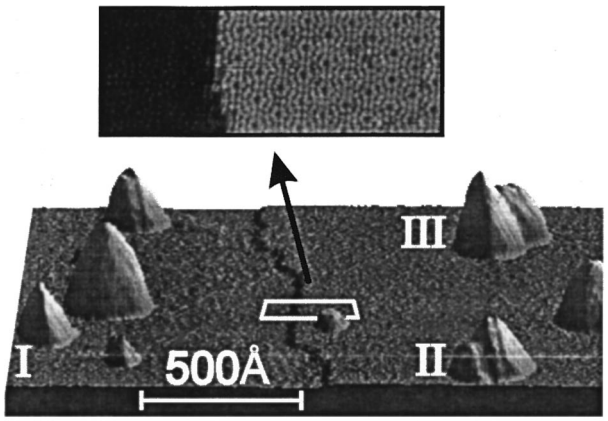

FIG. 2. Three-dimensionally rendered image of Si(111)-(7×7) onto which Ag nanocrystals have been deposited. The inset shows that the 7×7 reconstruction is preserved during Ag growth on Xe and Xe desorption. Structure I contains ~200 atoms, as in Fig. 1(b) and is 27 Å high. II represents a structure derived from two that had made contact upon reaching the surface. It is likely to be undergoing a shape change to reduce its surface energy. III is actually two separate structures that appear to touch. Their lateral sizes are exaggerated because they are imaged with the tip. There is no Ag-atom exchange among separated structures, and coarsening is not observed.

rent (20 nA), as discussed below. Structure III appears to be derived from two crystallites but, based on their heights and apparent footprints, these two are not in physical contact. Noncontacting features did not change in size or position with time or repeated scanning. Their stability against coarsening indicates that there was little atom exchange. Thus, the number of Ag atoms exchanging between the Ag nanostructures and Si(111)-(7×7) terrace sites is small at room temperature.

Figure 3 shows an area equivalent to Fig. 2 before and after pushing the nanocrystals with the tip. The white streaks are due to Ag atoms that have transferred to the surface. Such painting has been done in two ways. In one procedure, we scanned a large area in the imaging mode, as in Fig. 3(a), and then positioned the tip so that its path would cross the feature to be moved. A single line scan was then made with a fast scan speed (>10 μm/s), so that the feedback could not respond to avoid impact. When contact was established, the nanocrystal moved laterally with the tip, and the tip tried to retract. Normal scanning was then resumed for the retracting line scan. Figure 3(b) was obtained after the nanocrystals were modified, one by one, in the fast-approach mode, moving the tip from right to left. The tracks decrease in width because the contact area shrinks as material is transferred. The density of the Ag track was estimated from the total number of atoms of a cluster before and after a short distance ''nudge'' where we could measure both the change in height of the cluster and the area of the Ag track. This gave a planar density of $\sim 1.0\times 10^{15}$ atoms cm^{-2}. From results for more than 50 cluster manipulations, we conclude that the atoms in the tracks represent up to $\sim\frac{1}{3}$ of the atoms from the initial nanocrystal. The remainder have adhered to the tip. The features in the painted areas were ~1.6 Å higher than the Si adatoms.[10] The resolution of the image did not change much when a particle was nudged or picked up, implying that con-

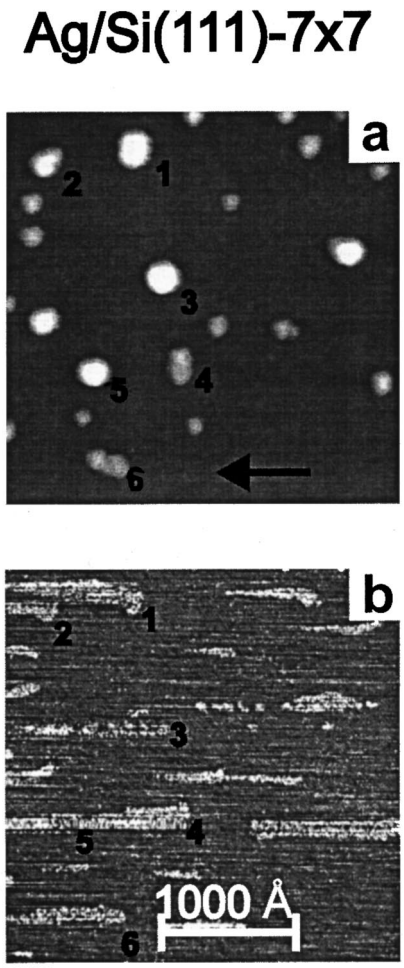

FIG. 3. (a) Distribution of Ag nanostructures, as in Fig. 2, before manipulation with the tip. (b) Tracks left by Ag nanostructures as they were moved by the tip. The numbers aid the eye in identifying the original positions in (a) and the track in (b). The arrow defines the direction of tip motion during the scan that established contact in the fast-approach mode. The distribution of Ag in the track indicates preferential transfer to the active sites of the 7×7 cell.

tact involved the shank and not the active tunneling tip. Equivalent results were obtained with a second approach that involved a single line scan at a slower scan speed (~1000 Å/s) with the feedback disabled to assure contact. The tip-to-surface distance was ~10 Å,[16] as in the fast-approach mode. Manipulation was also possible with structures derived from clusters that were in contact with each other but were still distinguishable, such as structure II in Fig. 2 or structure 6 in Fig. 3. Patterning could be done by selecting which nanostructures within an array would be painted and which would be left—and in what order (in Fig. 3, structure 5 was moved before structure 4). Nonlinear painting could be done by changing the scan direction relative to the sample in sequential nudging. The results for both fast-approach and fixed-height manipulation were reproducible with different tips and different samples. Moreover, painting could be done when the tip passed over the particle on center or off center. The overall irregularity of the painted line suggests complex dynamics of motion and contact.

TABLE I. Consequence of UHV manipulation of clusters derived from 100–40 000 atoms.

Cluster	Substrate	Substrate-cluster interaction	Result of manipulation
Ag	Si(111)-(7×7)	intermediate (increases with contact area)	Ag track created by adhesive wear, partial transfer to tip for $h<80$ Å
			Ag track created, cluster remained on surface for 80 Å$<h<$120 Å
			$h>120$ Å, no movement, tip crash
Cu	Si(111)-(7×7)	strong	no track, failure within cluster, partial transfer to tip
Ag+Cu	Si(111)-(7×7)	mixed	Ag track plus Cu clusters on surface, partial transfer to tip for <25-at. % Cu,
			no track, failure within cluster, partial transfer to tip, surface residue for >25-at. % Cu
Ag	Ag(111) and Si(111)-($\sqrt{3}\times\sqrt{3}$) Ag	strong	failure within cluster, partial transfer to tip, surface residue
Ag	vacuum-aged Si(111)-(7×7)	weak	adsorbates reduce adhesive wear, partial transfer to tip
Ag	Si(111) oxidized in air	weak	cluster removed without track, no wear
Ag	Br/Si(111)-(7×7)	weak	complete transfer to tip, no residue

The ability to move Ag nanostructures like these was dependent on their size because of the contact area and therefore the number of Ag-Si bonds. The contact area between the cluster and the Si(111) surface increased as the height of the cluster increased. Those whose heights were greater than ~120 Å (~200 000 atoms) could not be moved.[10] For them, the force of adhesion was large enough to resist movement by the tip, and the tip crashed. Those with heights of 80–120 Å (60 000–200 000 atoms) could be nudged and left tracks, and they remained on the surface. Structures whose heights were less than about 80 Å formed tracks but disappeared from the surface after pushing, as in Fig. 3. These results are summarized in Table I.

From the paint marks produced by manipulation, Ag-atom transfer occurs to the triangular areas bounded by the adatoms but not to the corner holes or the dimerized lines that border the unit cell.[10] This selective transfer is consistent with the fact that these areas are favored bonding sites when Ag atoms are deposited on Si(111)-(7×7) at low temperature.[17] Growth by atom deposition produces a dilute interface layer that preserves the 7×7 reconstruction but also produces a high-quality (111)-oriented Ag overlayer.[18] From our manipulation results, it is clear that Ag transfer to those active sites represents an energy gain relative to bonding to Ag. This occurs atom by atom, as can be envisioned from Fig. 1(b), as atoms hop from low coordination Ag sites to form Ag-Si bonds, sacrificing Ag-Ag bonds and introducing local strain. The fact that the track is only one layer in thickness indicates that transfer does not involve shearing processes in the Ag nanostructure.

Finally, Ag dots could be made on Si(111)-(7×7). This generally happened when nanocrystals were scanned under high tunneling current conditions (>20 nA). Under such conditions, the tip was much closer to the particle than under normal imaging, and contact is established somewhere on the tip shank [Fig. 1(c)]. Since the tip is following the height profile of the particle, however, contact with the particle is not as robust as that obtained in the fast-approach single-scan mode. Typically, it required several scans with high current to establish a sufficiently strong neck for removal to occur.

Cu nanocrystals and Si(111)

To investigate surface adhesion for a metal which has a greater tendency to react with Si(111)-(7×7) than does Ag, we used the buffer layer process to grow and deliver Cu nanocrystals. Figure 4 shows five nanocrystals grown by depositing 0.1 Å of Cu on 500 ML of Xe on Si. Before attempted manipulation, they were 18–26 Å in height (1000–3000 atoms)—smaller than in Figs. 2 and 3 because of the smaller amount of material. Figure 4 shows these same clusters after attempted manipulation using the fast-approach procedure that was successful for Ag. Nanopainting was not achieved. However, each Cu particle was modified by con-

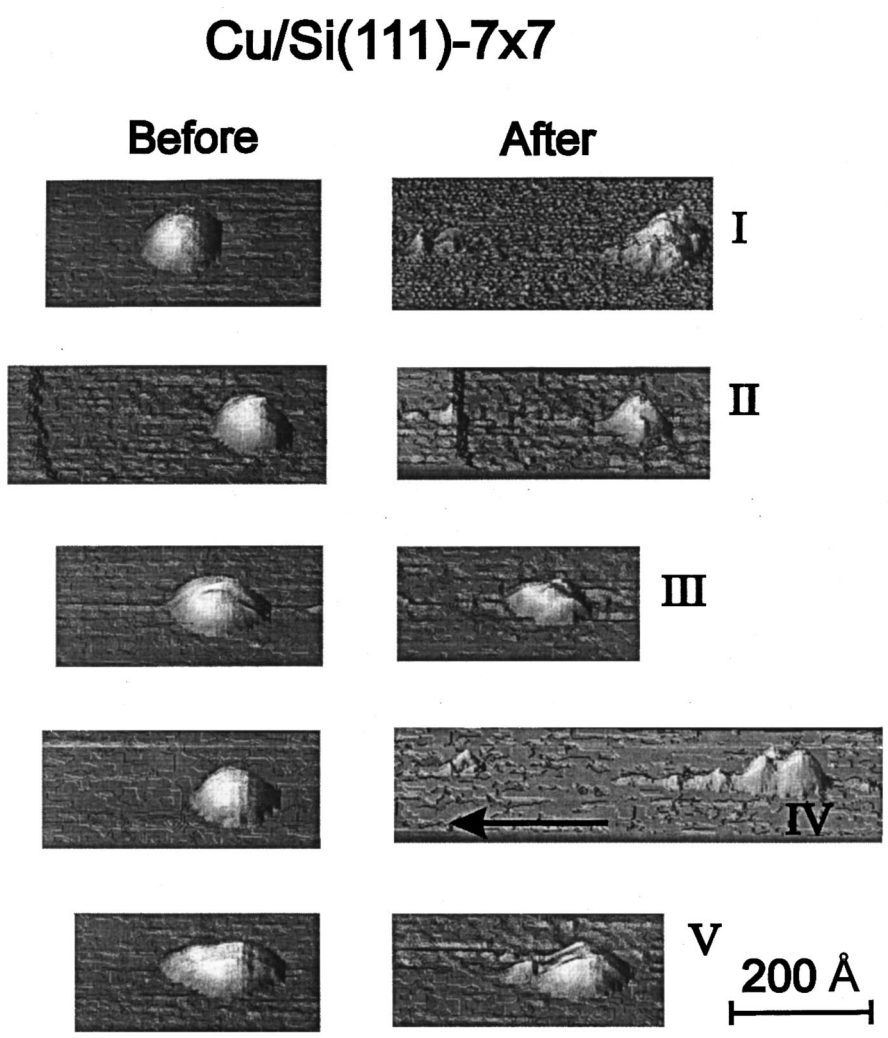

FIG. 4. STM images showing five Cu clusters on Si(111)-(7×7) before and after modification by the tip in the fast-approach mode. Strong Cu-Si bonding prevented manipulation and painting. Instead, they were reduced in heights as they were sheared. The debris along the path indicates that the sheared material transferred to the tip, but was deposited when the tip reapproached the surface.

tact because their heights were reduced to 8–13 Å. Structures I, II, and IV were broken into parts, and there was debris approximately at the end of the line scan. For structure II, the debris was close to a step. We conclude that contact with the tip exceeded the shear strength of the nanocrystal and that part of it was first attached to the tip but could be transferred to the surface when the tip reapproached the surface. These repeated contacts did not cause any visible changes in the quality of the images. In Table I, the substrate-cluster interaction is judged to be strong, in comparison to that for Ag.

The differences between manipulation of Ag and Cu nanocrystals on clean Si(111) reflects differences in interface bonding. For Cu-Si(111), the interface formed by atom deposition at room temperature exhibits significant intermixing as the 7×7 reconstruction degrades.[19] This disruption is driven by the tendency to produce structures having three-dimensional Cu-Si coordination. In this case, heating would produce Cu_3Si. For cluster deposition and relaxation at the surface, strong Cu-Si bonds can form, and limited intermixing involving adatoms may occur. Subsequent attempts to manipulate Cu particles must overcome these bonds, and this does not happen. Instead, the images show that failure occurs within the Cu particle as it is sheared. The interaction with the tip that could establish a neck is also different than for Ag. In particular, the surface free energy of Cu is comparable to that of W, and much higher than that of Ag, and this reduces the tendency to wet the tip.[20] Moreover, the activation energy for diffusion of Cu is greater than that of Ag. Weak bonding to the tip accounts for the deposition of fragments when the tip returns to the surface at the end of the line scan.

Cu-Ag nanocomposites and Si(111)

To explore the manipulation and adhesion of composite nanocrystals, we formed mixed structures of Cu and Ag. In this case, Ag was deposited onto 60-ML Xe to form clusters (average size of ~28 atoms[5]), and then Cu was added. These metals have little bulk solubility but their surface energies indicate that Ag would wet Cu.[20] Figure 5(a) depicts Ag clusters on Xe that form first. Also shown are separate Cu clusters and Cu that has contributed to the growth of a com-

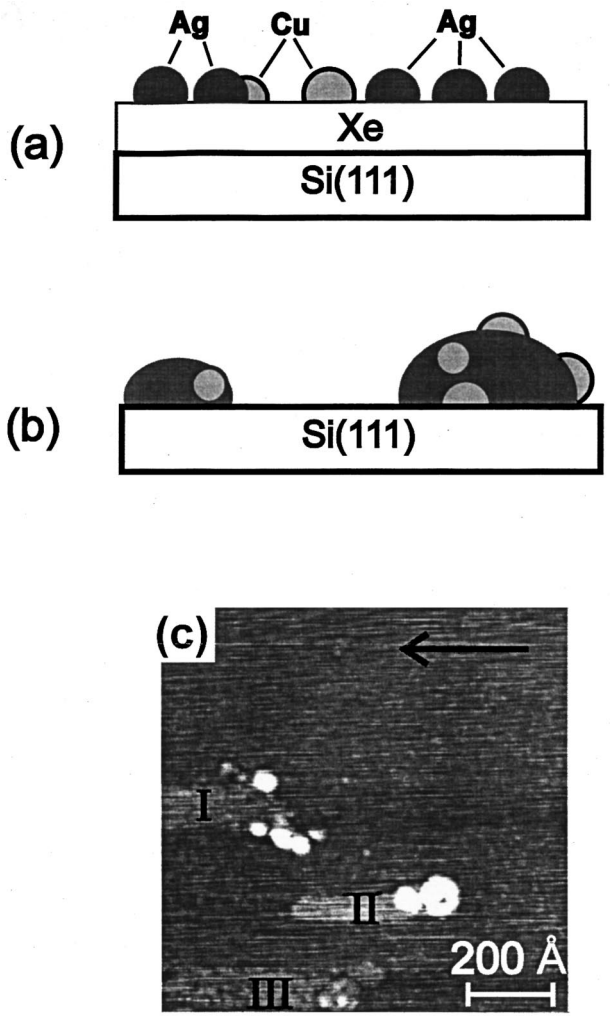

FIG. 5. (a) Depiction of the formation of an array of Ag clusters, Cu clusters, and Cu-Ag clusters on Xe after exposure to Ag and then Cu atoms from a thermal source. (b) Desorption of Xe agitates the clusters, and coalescence occurs when they contact each other. A cross section through one possible composite that has reached the Si(111)-(7×7) surface would show a nanostructure of predominantly Ag bonded to a smaller structure of Cu and wetting the copper. Another through a larger Ag nanostructure would show Cu decorating the outside, encapsulated within, and bonding to the Si surface. (c) Fast-approach manipulation of composite Ag-Cu particles grown by depositing 0.93-Å Ag and then 0.07-Å Cu resulted in painting due to the dominance by Ag. Small clusters close to the heads of the tracks are associated with Cu that had bonded to the Si surface and had been selectively separated from the moving Ag.

posite structure. Depending on the number and make-up of clusters that coalesce during Xe desorption, we would expect to find composites on the Si(111)-(7×7) surface like those shown in cross section in Fig. 5(b). Both are Ag rich. The one on the left is small, and Ag has wetted the Cu particles. The one on the right has grown to substantial size with one Cu cluster incorporated, one touching the Si surface, and two at the outside. Mixed structures like these are a consequence of their formation process. Once in contact with the Si surface, we would expect different reactivities for Cu and Ag, constrained by kinetics. Structural rearrangements associated with contacting and wetting will result in mixed interface bonding, again subject to atom diffusion. If these mixed structures were to be heated, then we would expect to see areas of Cu-Si and areas with Ag-Si products, depending on the thermodynamic state achieved.

Figure 5(c) shows the consequences of manipulation for structures grown from 0.93-Å Ag and 0.07-Å Cu.[21] The initial cluster density was 5×10^{10} cm^{-2}, and the heights ranged from 9 to 80 Å. There was nothing distinctive about the starting clusters that would reveal their compositional makeup. Manipulation resulted in Ag painting but, in contrast to pure Ag, there was also residual material near the starting position. Line I, for example, shows five clusters 3–7 Å in height near the beginning of the track. The initial height of the composite was 55 Å. The end of the track corresponds to the point where transfer to the tip occurred. It is reasonable to associate the track with Ag and the small features to Cu. Line II was produced by defining the end of a fast-approach line scan to be ~400 Å beyond a nanocrystal whose initial height was 28 Å. After contact, the larger residual cluster was 8.5 Å. The rest of the particle adhered to the tip. While equivalent short lines and cluster pickup was observed for pure Ag, there was no material left at the start of the line. We propose that the two components of the composite in lines I and II were separated by their different affinities to bond to Si(111) and the tip. This separation is not complete because the volume of the leftover material is insufficient to account for the amount of Cu deposited. Thus, some Cu will have transferred to the tip along with the Ag. Line III is a result of painting with a nanocrystal 33 Å in height. Painting was successful but the moving structure eventually adhered to the tip. At the original site of the structure, we see two small clusters of ~3-Å height. We cannot unambiguously identify their elemental make-up but note again that such debris was unusual for pure Ag painting.

Composite nanostructures could be produced with any relative amount of Cu, but attempts to nudge or paint failed for compositions exceeding 25-at.% Cu. Instead, features similar to those of pure Cu were obtained. The complex morphology of the as-formed composite would make it unlikely that the tip could extract the Ag. In principle, Ag could wet larger Cu clusters to form a sacrificial lubricant, but the Ag mobility on Cu is likely to be the limiting factor for extensive wetting.

Ag nanostructures on modified Si surfaces

The balance between surface and tip adhesion for Ag particles is sensitive to the cleanliness of the Si(111)-(7×7) surface. To investigate this, we formed a nanostructure array, as in Fig. 3(a), on a freshly prepared Si surface. Manipulation with the tip was successful, as in Fig. 3(b). The sample was then aged *in vacuo* for ~70 h to allow adsorbate accumulation at the chemically active surface sites. For these adsorbate-decorated surfaces, we were unable to resolve the 7×7 reconstruction with STM. Under these conditions, the Ag particles transferred more readily to the tip, and the likelihood of painting was greatly reduced; see Table I. In effect, residual gas adsorption reduced the ability of the nanopar-

ticles to bond to Si(111) while necking with W was less affected. Note that footprints at the initial positions of the particles were still evident.

In another experiment, we dosed Si(111)-(7×7) with Br at 300 K.[22] Ag nanostructures that were delivered to this surface were unstable under our imaging conditions. Scanning had the effect of removing the Ag, and we conclude that it transferred to the tip. Hence attraction to the tip through necking was strong and adhesion to the surface was insufficient to assure contact. This is reasonable since monovalent Br would saturate the Si dangling bonds so that Ag bonding and transfer is frustrated. (Heating this Ag-Br-Si surface produced AgBr crystallites.)

In a third experiment, we explored the possibility that nanostructures formed by buffer-layer-assisted growth could be manipulated after being exposed to air. In this case, Ag structures were deposited on Si(111)-(7×7), as in Fig. 3(a), and then exposed to air to oxidize the Si surface and modify the Ag particles. These particles could be imaged with an atomic force microscope, using the soft-tapping noncontact mode and an etched Si tip. They could also be moved with higher-amplitude tapping, and areas could be swept free of Ag. During manipulation, they remained on the oxidized surface, and they moved without leaving tracks that could be seen with the AFM. Such manipulation occurs under conditions where surface bonding is weak and necking is negligible. It is analogous to that of Ref. 6, though buffer-layer-assisted growth introduces control over the particle size and increases the range of its elemental makeup.

The interaction of Ag with clean Si was varied in another way by changing the surface reconstruction to Si(111)-($\sqrt{3}\times\sqrt{3}$) Ag. This was done by depositing 20 Å of Ag onto Si(111)-(7×7) and heating to 700 K. This produces two lower energy structures, namely, Ag(111) crystallites and large areas of Si(111)-($\sqrt{3}\times\sqrt{3}$) Ag. The $\sqrt{3}\times\sqrt{3}$ reconstruction contains 1 ML of Ag positioned slightly above a half-bilayer of Si atoms arranged into trimers. In this structure, each Ag atom has four Ag neighbors and one bond to the Si atoms at the corner of each Si trimer.[23] Subsequent delivery of Ag nanostructures produced features equivalent to those of Fig. 3(a). Attempts to move them with the STM tip were unsuccessful, but the upper portions of the nanocrystals were removed from the main body through a nanoshearing process. Such intraparticle failure indicated that the Ag nanostructure itself was the weak link relative to bonds to the tungsten tip and the Si(111)-($\sqrt{3}\times\sqrt{3}$) Ag surface.

With these two-phase samples, we were also able to examine the stability of Ag nanocrystals delivered to Ag(111). Images obtained shortly after delivery showed multilayer (111) islands with hexagonal footprints that corresponded to ⟨110⟩ steps. Neither nanopainting nor removal was possible for these particles. Impact with them did result in shearing but the base remained intact. Imaging before and after impact indicated a reduction in height as material was transferred to the tip. A series of images of the same portion of the surface showed that 3D islands decayed into monolayer high islands and that these islands coarsened. Such coarsening is consistent with the high diffusivity of Ag on Ag(111) and the low barrier for atom hop-down (interlayer transport). Approach to the equilibrium final state was readily observed at 300 K, as has been discussed elsewhere.[24]

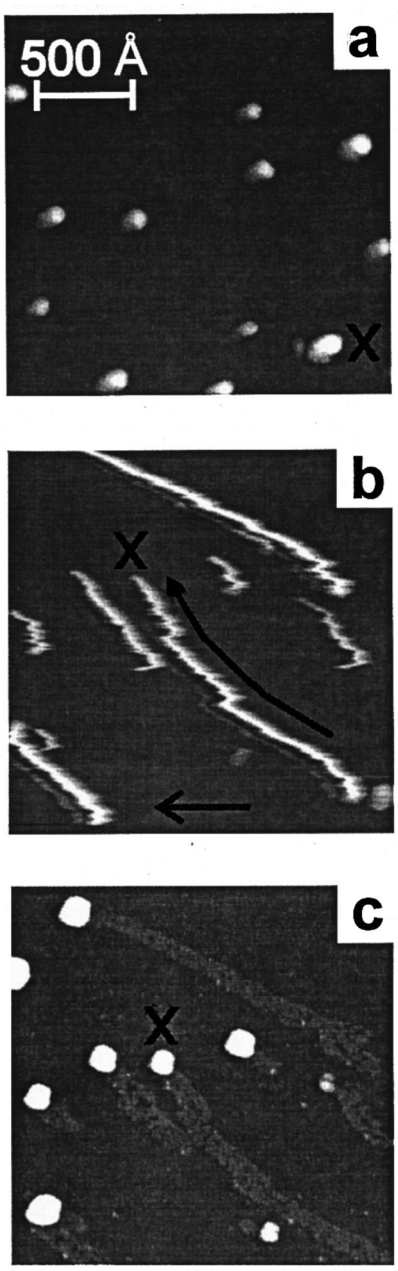

FIG. 6. (a) Distribution of Ag nanocrystals on Si(111)-(7×7) imaged with 0.2-nA current. (b) Image derived from line scans at 20-nA current. Weak contact with the nanostructures causes them to ''dribble'' away with each successive line scan. The arrow identifies the path of structure *X*. Eventually, particle motion is arrested, and the tip passes over it. (c) Image acquired with 0.2 nA showing the location of the arrested Ag particles and the tracks created by adhesive wear during movement by the tip.

High-current manipulation of Ag nanocrystals on Si(111)-(7×7)

The above discussion of Ag painting on Si(111)-(7×7) emphasized manipulation by tip contact. A different kind of painting can be achieved by increasing the tunneling current from 0.2 to 20 nA at +2-V bias. In this case, there is inter-

mittent contact with the nanocrystal while the tip is scanning. This is a more delicate form of manipulation than that of high-speed impact.

Figure 6 shows the effect of high-current scanning for an array of nanocrystals obtained after depositing 0.2-Å Ag on 60 ML of Xe. The features evident in Fig. 6(a) ranged in height from 20 to 46 Å, and feature *X* was 46 Å high. They were smaller than those of Fig. 3 because less Ag was initially deposited. After obtaining Fig. 6(a), the tunneling current was increased from 0.2 to 20 nA. Scanning at high current produced images that showed white streaks [Fig. 6(b)], that indicated the positions of the nanocrystals as the tip moved them. Imaging at 0.2-nA current revealed the positions of the cluster array without disturbing them [Fig. 6(c)].

This high-current form of pushing is analogous to dribbling a soccer ball with the side of the foot. With each line scan, the tip comes very close to a Ag particle, establishing contact, and the particle is bumped away. In these scans, the tip moves along a line from right to left, and then retraces that line before advancing upward by one line. No data acquisition takes place during the retracing movement, but contact can be made. This explains why the particles sometimes appear to move to the right. With each right-to-left scan, the tip ''sees'' the retreating features. From Fig. 6(b), this dribbling is not 100% successful. In particular, feature *X* has advanced with the tip but it is arrested about two-thirds of the way to the top of the image. We can speculate that this jump over the particle is due to a change in the tip itself as a new active tunneling point is established. During dribbling contact, nanocrystals do not transfer to the tip, though they are as small as 20 Å in height (~1000 atoms).

The fast-approach manipulation mode is reproducible with different tips and samples, as noted above. The dribbling mode is more dependent on the tip profile because the contact is more subtle. We speculate that dribbling occurs under conditions that do not favor neck formation, perhaps hindered by impurities on the tip. Such tip-sample mechanical interaction is still largely unexplored.[25] It is possible that nanopainting with the dribbling mode can be improved by using a tip with lower surface energy than the nanocrystal or by passivating the tip.[26]

Finally, Fig. 7 shows two Ag clusters that were ~100 Å apart. Based on their heights, they were not in contact when first imaged at 0.2-nA tunneling current, top. Scanning four times at 20 nA produced a change in shape, when observed under normal imaging conditions, bottom. Such tip-induced coalescence was successful only when the scan direction was along the internuclear cluster axis, indicating that the tip nudged one cluster toward the other and contact occurred. Shape changes that lowered the surface energies were then assisted by high current and tip bumping. Such merging was done under ultrahigh-vacuum conditions, and coalescence was thermodynamically favored. Merging was observed for cluster heights between 20 and 110 Å and separations up to 400 Å.

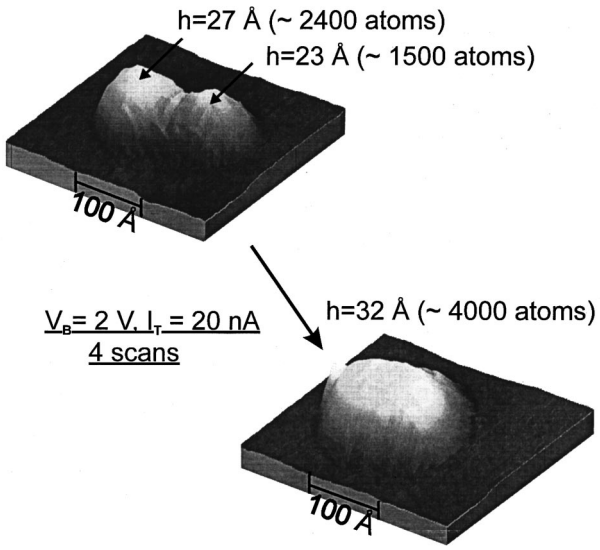

FIG. 7. Two A particles ~100 Å apart on Si(111)-(7×7) were imaged at low current, top, and then scanned four times at 20-nA current. This scan direction was along the internuclear axis. The tip caused the two structures to come into contact and to coalesce.

CONCLUSIONS

With buffer-layer-assisted growth, it is possible to produce atomically clean nanocrystals of a wide variety of sizes and to bring them into contact with equally clean surfaces. Interface intermixing of the sort associated with atom deposition and overlayer growth is minimized, and a unique solid-solid contact is established. This procedure can be followed for a wide range of materials.

In this paper, we used a STM tip to manipulate, modify, and remove clusters from surfaces that were atomically clean or intentionally altered to alter the local chemical interactions responsible for adhesion. As summarized in Table I and discussed in the text, the results depended on the bonding with the substrate and with the tip. The contact between Ag and Si(111)-(7×7) was relatively weak, and the particles could be moved even if they were derived from tens of thousands of atoms. Associated with this movement was the transfer of Ag atoms to the Si surface to selectively form Ag-Si bonds. This represents adhesive wear. For Cu particles, the interface bonding was stronger and manipulation was not possible. For Ag deposited onto Ag(111), there was wetting, the formation of multilayer islands, and the decay of the islands because of high atom mobility on Ag terraces. In contrast, clusters deposited onto Si(111)-derived surfaces were trapped in higher-energy states because atom exchange was minimal.

Future studies will expand the scope of those discussed here. They will consider the formation and the compatibility of particles of nanoscopic dimension (with hundreds to thousands of atoms) with metal and semiconductor surfaces.

ACKNOWLEDGMENTS

This work was supported by the Office of Naval Research. We thank K. Nakayama and B.-Y. Han for stimulating discussions.

[1] D. M. Eigler and E. K. Schweizer, Nature (London) **344**, 524 (1990).
[2] I.-W. Lyo and Ph. Avouris, Science **253**, 173 (1991).
[3] Y. Z. Li, M. Chander, J. C. Patrin, J. H. Weaver, L. P. F. Chibante, and R. E. Smalley, Phys. Rev. B **45**, 11 387 (1992).
[4] L. Bartels, G. Meyer, and K.-H. Rieder, Phys. Rev. Lett. **79**, 697 (1997).
[5] W.-W. Pai, Z. Zhang, J. Zhang, and J. F. Wendelken, Surf. Sci. Lett. **393**, L106 (1997).
[6] D. M. Schaefer, R. Reifenberger, A. Patil, and R. P. Andres, Appl. Phys. Lett. **66**, 1012 (1995); T. Junno, K. Deppert, L. Montelius, and L. Samuelson, *ibid* **66**, 3627 (1995); C. Baur, B. C. Gazen, B. Koel, T. R. Ramachandran, A. A. G. Requicha, and L. Zini, J. Vac. Sci. Technol. B **15**, 1577 (1997).
[7] H. J. Mamin, P. H. Guethner, and D. Rugar, Phys. Rev. Lett. **65**, 2418 (1990); S. E. McBride and G. C. Wetsel, Jr., Appl. Phys. Lett. **59**, 3056 (1991).
[8] T.-C. Shen, C. Wang, G. C. Abeln, J. R. Tucker, J. W. Lyding, Ph. Avouris, and R. E. Walkup, Science **268**, 1590 (1995).
[9] L. J. Whitman, J. A. Stroscio, R. A. Dragoset, and R. J. Celotta, Science **251**, 1206 (1991).
[10] S. J. Chey, L. Huang, and J. H. Weaver, Appl. Phys. Lett. **72**, 2698 (1998).
[11] G. D. Waddill, I. M. Vitomirov, C. M. Aldao, and J. H. Weaver, Phys. Rev. Lett. **62**, 1568 (1989); J. H. Weaver and G. D. Waddill, Science **251**, 1444 (1991).
[12] L. Huang, S. J. Chey, and J. H. Weaver, Phys. Rev. Lett. **80**, 4095 (1998).
[13] J. W. Bartha and M. Henzler, Surf. Sci. **160**, 379 (1985). Correcting the ion gauge reading for its sensitivity to Xe, and assuming a sticking coefficient of unity at 25–52 K, gives a growth rate of 1 ML per 10-L exposure, where 1 ML is the atom density of Xe(111) and 1 L is 10^{-6} Torr sec.
[14] D. W. McComb, B. A. Collings, R. A. Wolkow, D. J. Moffatt, C. D. MacPherson, D. M. Rayner, P. A. Hackett, and J. E. Hulse, Chem. Phys. Lett. **251**, 8 (1996).
[15] G. D. Waddill, I. M. Vitomirov, C. M. Aldao, S. G. Anderson, and J. H. Weaver, Phys. Rev. B **41**, 5293 (1990).
[16] R. S. Becker, J. A. Golovchenko, D. R. Hamann, and B. S. Swartzentruber, Phys. Rev. Lett. **55**, 2032 (1985).
[17] Atom deposition onto Si(111)-(7×7) at room temperature produces a dilute monolayer with features that are 0.5–1 Å high. [St. Tosch and H. Neddermeyer, Phys. Rev. Lett. **61**, 349 (1988)].
[18] H. Hong, R. D. Aburano, D.-S. Lin, H. Chen, and T.-C. Chiang, Phys. Rev. Lett. **68**, 507 (1992).
[19] E. Daugy, P. Mathiez, F. Salvan, and J. M. Layet, Surf. Sci. **154**, 267 (1985); A. T. Ibrahimi, V. Mercier, C. A. Sebenne, D. Bolmont, and P. Chen, *ibid*. **152/153**, 1228 (1985).
[20] The surface energies of Cu(111), Ag(111), and W(110) are 2554, 1693, and ~3000 erg cm^{-2}. See R. Kern, G. Le Lay, and J. J. Metois, in *Current Topics in Materials Science*, edited by E. Kaldis (North-Holland, Amsterdam, 1979), Vol. 3, Chap. 3, pp. 131–420.
[21] The amounts of Ag and Cu are expressed in Å where 2.36 Å represents 1 ML of Ag(111) and 2.08 Å for Cu(111).
[22] R. J. Pechman, X.-S. Wang, and J. H. Weaver, Phys. Rev. B **52**, 11 412 (1995).
[23] I. M. Katayama, R. S. Williams, M. Kato, E. Nomura, and M. Aono, Phys. Rev. Lett. **66**, 2762 (1991); J. Nogami, K. Wan, and J. C. Glueckstein, Jpn. J. Appl. Phys. **33**, 3679 (1994). The transformation temperature is ~240 °C.
[24] S. Jay Chey, L. Huang, and J. H. Weaver, Surf. Sci. **419**, L100 (1998).
[25] J. Tersoff and N. D. Lang, in *Scanning Tunneling Microscopy, Methods of Experimental Physics*, edited by J. A. Stroscio and W. J. Kaiser (Academic, New York, 1993), Vol. 27, pp. 24–27.
[26] S. A. Joyce, R. C. Thomas, J. E. Houston, T. A. Michalske, and R. M. Crooks, Phys. Rev. Lett. **68**, 2790 (1992).